IMPACT OF ALUMINIUM PHOSPHATE ADDITION TO REFRACTORY CASTABLES ON SPINEL FORMATION WITH MOLTEN ALUMINIUM ALLOY

Wanja Reichert[1], Thorsten Tonnesen[1], M. Miriuta[2], Lise Loison[1], Rainer Telle[1]
[1]Institute of Mineral Engineering, RWTH Aachen, Germany
[2]ENSCI Limoges, Limoges, France

ABSTRACT
Refractories used in the aluminium industry undergo severe corrosion due to reaction with molten aluminium. The high wettability by aluminium melt is suspected to be a key factor for degradation and infiltration, hence anti-wetting additives such as $BaSO_4$, CaF_2 or $AlPO_4$ are added to the refractory to limit the contamination of the melt. The conditions as well as the mechanisms of the improved corrosion resistance are not yet well understood. In particular the behaviour of phosphor at the interface between refractory and aluminium melt is subject of current research. The present work aims at improving the corrosion resistance against molten aluminium of an alumina based no cement castable (NCC) as well a low cement castable (LCC) with addition of $AlPO_4$. It has been shown that for an anti-wetting effect a high amount of 10 wt.-% $AlPO_4$ is needed. Furthermore the use of additives leads to worsening the refractory microstructure especially when sintered at high temperatures, presumably due to rheological issues. Nevertheless, an improved corrosion resistance was obtained in static crucible test even at fewer addition of $AlPO_4$ around 6 wt.-% presumably due to the formation of high-temperature phases like spinel. This study intends to examine the impact of varying $AlPO_4$ addition to an alumina low and no cement castable to the MA-spinel and other high-temperate phase formation at the interface between aluminium alloy Al 7075 and the refractory castable. The applied methods include a first characterization of the material, examination of spinel formation mechanisms by SEM and XRD as well as a study of the reactivity with aluminium melt during a dynamic laboratory finger test according to standard CEN/TS 15418. The efficiency of the addition and its impact on the microstructure including Young's Modulus as well as the possible improvement of the infiltration resistance are discussed.

Keywords: aluminium melt, corrosion, $AlPO_4$, sol-gel, castables, infiltration resistance

INTRODUCTION

Corrosion with aluminium melt

Aluminium melts are well known for their extreme reducing behaviour towards refractories. The corrosion mechanisms of commonly used aluminosilicate or high alumina refractories have been the focus of several studies [1,2]. Especially modern alloys with constituents of zinc and magnesium have a severe impact of the degradation on the furnace lining. As aluminium alloys become more complex the materials suitable for aluminium melts are limited. The optimization of refractory composition for applications in contact with aluminium has focused on the use of non-wetting additives in order to reduce aluminium attack and metal penetration into the refractory. [3] Furthermore recent studies tend to focus on bonding systems such as phosphate bonds [4] or sol binders. [5,6]

Phosphates as non-wetting additives

The optimization of refractory composition for applications in contact with aluminium has focused on the use of non-wetting additives in order to reduce aluminium attack and metal penetration into the refractory like $BaSO_4$, AlF_3 and CaF_2. Those compounds are added to the castable matrix to reduce the wettability and the reactivity with aluminium melt. $AlPO_4$ is mostly used as a binder, as phosphate binders show the best high temperature properties. However, Firoozjaei et al. also examined the influence of this component as a non-wetting additives to an andalusite low cement castable composition. [3]

Phosphate bonds

As previously mentioned, phosphate bonds are one of several bonding systems especially for high temperature applications. The effect of mixing hydraulic and phosphate bonds in refractory LCC castables revealed a positive effect on cold crushing strength when mixed with alumina-spinel as basic material. The presence of calcium phosphate is supposed to support the formation of high-temperature phases as spinel or magnesium phosphate. [4]

Sol-gel bonding system

With an increased demand of low cement monolithic refractories the demand of an alternative, non-hydraulic bonding system increased. A promising approach are sol-gel binding systems due to the wide range of possible applications. Sol is a metastable condition and comprises fine colloidal particles mostly of the same composition as the castable. While curing it forms a network of gel-structure, depending on variation of pH, time and temperature and develop ceramic bonding through sintering. Furthermore, the sol does not need an addition of a deflocculant. Nevertheless, the high costs of the precursors limit the wide use of sol-gel binders in refractory materials. [5,6]

EXPERIMENTAL PART

Materials

Two different high alumina refractories were produced: A low cement castable (LCC) with maximum grain size of 3 mm with a free flow deflocculant dissolved in water and a sol-gel based no cement castable (NCC). The alumina sol was prepared from a commercial boehmite powder containing acetate. No water addition was needed, due to the presence in the sol with a solid content of 10 wt.-%.

Three formulations of the LCC and five formulation of the NCC with different amounts of $AlPO_4$ were studied. The aluminium phosphate was added by substitution of tabular alumina based on the same solid content as the reference castable (without $AlPO_4$) at a rate of 1 and 10 wt.-% to the LCC and 1, 3, 6, 10 wt.-% to the NCC. Based on the particle size distribution of the $AlPO_4$ commercial powder, the substitution of tabular alumina and reactive alumina grain size with AlPO4 powder was optimized in order to approach the initial distribution of grain size and keep the compactness of the packing constant for all composition (Table 1). The prismatic bars (150*25*25 mm^3) of the LCC cured during 48 h in a humid chamber the NCC cured on air. Both were then dried at 110 °C for 24 h and sintered at 1500 °C for 6 h.

All high alumina raw materials (sintered Al_2O_3) are provided by **Alteo**. The cement used in the LCC composition is supplied by **Kerneos**. FS 65 deflocculant provided by **BASF**.

Tab. 1. Composition of the tested castables

Raw material	Type	Sol-gel									
		REF	P1	P3	P6	P10	REF	P1	P3	P6	P10
		[wt.-%]					[wt.-%]				
Reactive alumina	**PFR**	14,0	13,8	13,4	12,8	12,0	12,5	12,5	12,5	12,5	12,5
Tabular Alumina	**0 – 0,045 mm**	12,5	12,1	11,3	10,1	8,5	10	9,5	8,5	7,0	5,0
	0 – 0,3 mm	10	9,7	9,1	8,2	7,0	17,5	17,1	16,3	15,1	13,5
	0,2 – 0,6 mm	10,5	10,4	10,2	9,9	9,5	10	9,9	9,7	9,4	9,0
	0,5 – 0,1 mm	17,5	17,5	17,5	17,5	17,5	10	10	10	10	10
	1 – 3 mm	35	35	35	35	35,0	35	35	35	35	35
CA Cement	**CA Secar 71**						5	5	5	5	5
Sol	**Boehmite**	6,5	6,5	6,5	6,5	7,5					
	AlPO4	0,0	1,0	3,0	6,0	10,0	0,0	1,0	3,0	6,0	10,0

Properties

Young's Modulus was measured according to ASTM C 1548-02 (2012) by Resonance Frequency Damping Analysis (RFDA) equipment. This device enables a non-destructive test, which measures and determines the frequencies of the sample's acoustic emission further to a mechanical impulse. Finally Young's Modulus is calculated in flexural mode and is confirmed with a measurement in longitudinal mode.

The corrosion resistance of the samples against aluminium attack is evaluated via the static crucible test as well as by the dynamic finger test according to CEN/TS 15418:2006 (D), with the aluminium alloy 7075 (90% Al – 5,1% Zn – 2,1% Mg – 1.2% Cu – 0,5% Fe – 0,4% Si – 0,3% Mn – 0,18% Cr – 0,2% Ti). The crucible corrosion test is performed for a four-day period at 1000°C and published elsewhere. [8] Finger tests are performed at the same temperature with an immersion time of 6h while rotated with ten rotations per minute. Upon the completion of the test, samples were cooled to room temperature and cut across a diagonal plane, in order to observe the extent of the corroded area and the penetration depth of aluminium.

For better understanding of the interaction between the molten alloy and the refractories, X-ray diffraction measurements (XRD) were conducted. Microstructural analyses were elaborated by scanning electron microscopy (SEM) as well as chemical composition via energy dispersive X-ray spectroscopy (EDX)

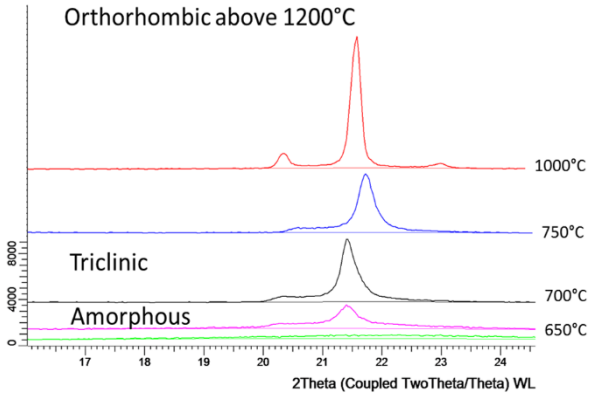

Fig. 1: XRD results of $AlPO_4$ sample after thermal treatment from room temperature (bottom) up to 1000°C (top)

RESULTS AND DISCUSSION

Material characterisation

Figure 1 shows the XRD pattern of an $AlPO_4$ sample, added to the refractories from room temperature up to 1000°C. The amorphous $AlPO_4$ can be observed until a temperature of 550°C. At a temperature of 650°C a triclinic $AlPO_4$ phase can be detected. With increasing temperature the peak of the triclinic $AlPO_4$ is increasing. Above 1200°C the sample undergoes an irreversible crystallographic phase change from triclinic to the orthorhombic structure.

After sintering at 1500°C for 6h the orthorhombic $AlPO_4$ is present in all castables with 10wt-% $AlPO_4$ addition, however the XRD pattern shows the presence of both triclinic $AlPO_4$ and orthorhombic $AlPO_4$ in the sol-gel bonded samples, hence an incomplete phase transition can be implied. Moreover an additional $Al(PO_3)_3$ phase was detected. (Figure 2)

In the LCC the added $AlPO_4$ reacts with the calcium provided by the cement to form calcium aluminium phosphate, therefore in all other LCC samples no $AlPO_4$ phases can be observed. There was no evidence of a reaction between $AlPO_4$ and Al_2O_3. The amount of corundum however is slightly higher in the NCC due to the addition of boehmite.

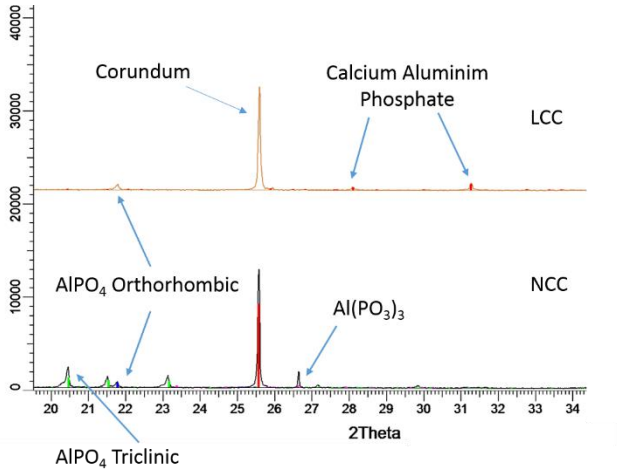

Fig. 2: XRD pattern of the LCC and NCC sample with 10 wt.-% $AlPO_4$ addition after sintering at 1500°C

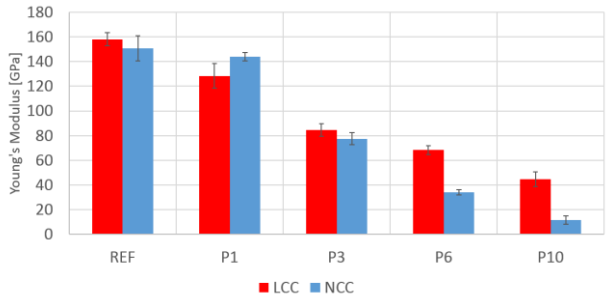

Fig. 3: XRD pattern of the LCC and NCC sample with 10 wt.-% $AlPO_4$ addition after sintering at 1500°C

The polymorphic phase transition of $AlPO_4$ during sintering corresponds with a change in volume, thus resulting in a crack network in the samples. Therefore a decrease of Young's Modulus can be observed with increasing aluminium phosphor amounts. The REF samples both of the NCC and the LCC exhibit the highest Young's Modulus with similar values of 158.4 GPa for the LCC and 150.8 GPa for the NCC respectively. Highest difference of values can be seen for samples P6 and P10, where Young's Modulus of the LCC are considerably higher. Nevertheless, both compositions attain relatively low mechanical strength.

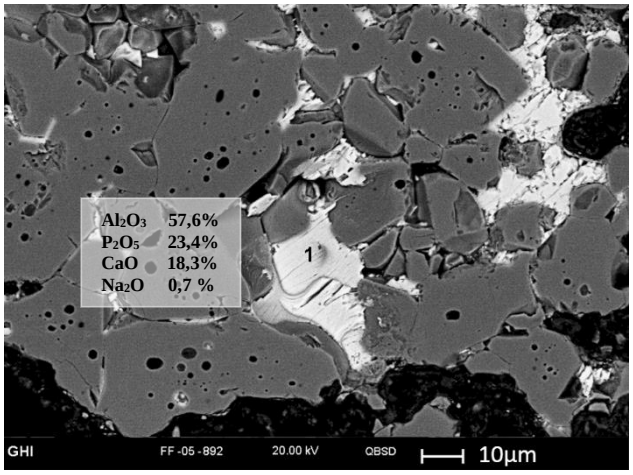

Fig. 4: SEM micrograph, castable LCC-P10: microstructure of sintered sample

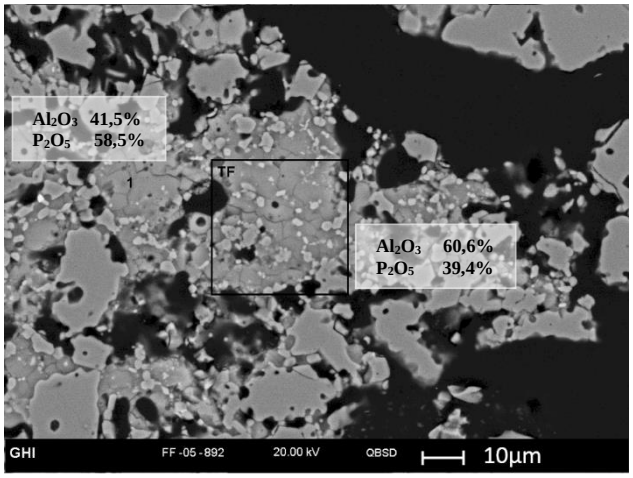

Fig. 5: SEM micrograph, castable NCC-P10: microstructure of sintered sample

Figure 4 and 5 show SEM micrograph of the phosphate rich phases of castable LCC-P10 and NCC-P10 after sintering. In Figure 4 an accumulation of calcium phosphate is observed nesting between the tabular alumina grains. Figure 5 shows, unlike the LCC, the phosphorous in the sol- gel bonded sample is scattered among the matrix, leading to a better phosphorous distribution in the sample. Discovered phases underline the XRD measurements mentioned above.

The high porosity especially in the NCC sample is mentionable and can illustrate the poor performance in Young`s Modulus measurement. It can be assumed that as long as calcium is present, the phosphor tends to react to form calcium phosphate resulting in less polymorphic phase transition of the $AlPO_4$ and lesser porosity. However a hyper-stoichiometric presence of $AlPO_4$ will lead to the formation of orthorhombic $AlPO_4$ phases.

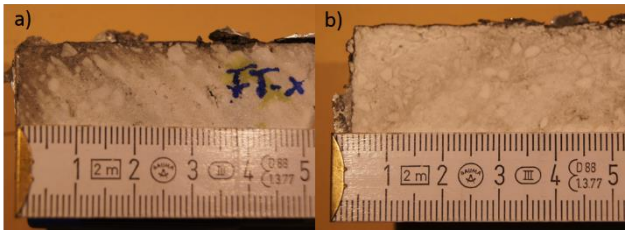

Fig. 6: Samples a) P10-LCC and b) P10-NCC after fingertest at 1000°C for 6h

Despite the extreme porosity previous studies illustrate the excellent corrosion resistance of the NCC under static conditions [8]. Therefore a dynamic finger test was conducted to evaluate and confirm the results under dynamic conditions. In figure 6 the P10 samples of both formulations can be seen after corrosion test. Besides the low mechanical strength both composition show good corrosion resistance. No erosion is visible, however infiltration up to 5 mm into the LCC sample can be seen. In contrast the NCC sample appears to be virgin.

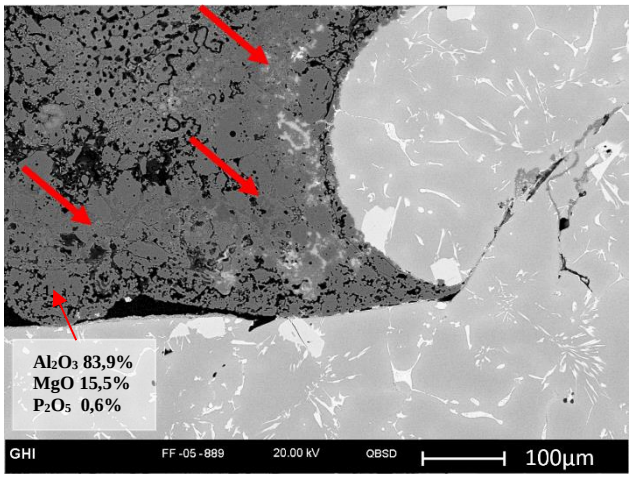

Fig. 7: SEM micrograph, interface castable NCC-P10 and alloy 7075: Spinel formation

The SEM analysis however revealed an interaction between refractory material and the molten aluminium alloy. In figure 7 the infiltration of the alloy into a micro pore is observable. Despite the high surface area, no deep infiltration into the refractory is apparent. The initial microstructure of the refractory can be seen about 200µm rewarded the metal-refractory interface. A thin spinel layer of more or less 100µm is merely seen at the interface, indicated by the red arrows. EDX measurements reveal small amounts of phosphor in the dense spinel layer.

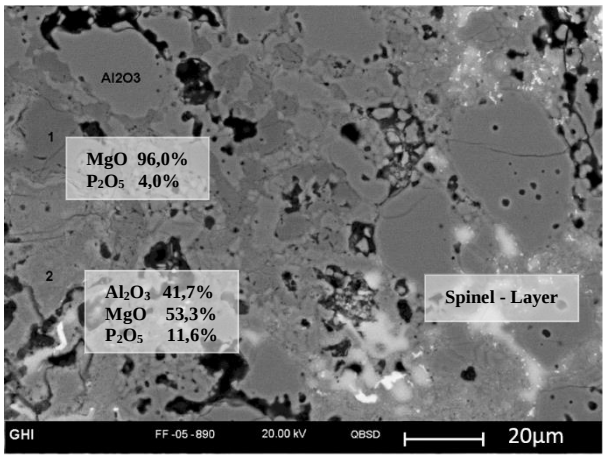

Fig. 8: SEM micrograph, castable NCC-P10 and alloy 7075: Magnesium phosphate and spinel formation

An increase of P_2O_5 up to 11.6 wt.-% concentration can be observed on deeper examination of and behind the spinel layer. Figure 8 shows a SEM micrograph around 150µm into the refractory from metal interface. Additionally a periclas phase with small amounts of magnesium phosphate phase is apparent which indicates a penetration of magnesium into the refractory material. As magnesium is only present in the aluminium alloy it can be assumed that all magnesium containing phases result from interaction between the molten aluminium and refractory material. Suprisingly no interaction is visible between the tabular alumina grains and infiltrated magnesium, so it is implied that infiltrated magnesium reacts with the phosphor hence do not react with the tabular grains. The order of spinel formation is subject of further investigations to clarify if magnesium is able to diffuse further into the refractory or if the reaction between the magnesium und phosphor precedes the spinel formation. Previous studies revealed a reinforcing effect of the microstructure due to the formation of magnesium phosphate [4] resulting in better erosion resistance.

Conclusion

The effect of $AlPO_4$ addition on high alumina low cement and sol-gel bonded no cement castable was examined. The formulation of the castables was calculated from the reference castable in order to maintain a similar grain size distribution through the weight additions of $AlPO_4$. First the study focused on the behaviour of amorphous aluminium phosphate, both as individual sample and in combination with the castable matrixes. The phase transition during heating as well as the reaction with matrix components was investigated. Young's Modulus measurements were carried out to test the change in mechanical behaviour due to alteration of the matrix. SEM micrographs and EDX measurements were taken to assist attained results.

With increasing concentration of $AlPO_4$ an increase of porosity and decrease of Young's Modulus was detected, nevertheless an increase of corrosion resistance was observed, especially for the NCC castable. Scanning electron microscopy measurements revealed that the formation of a thin spinel layer at the interface between molten alloy and refractory protects the matrix of further infiltration. Furthermore, the infiltrated magnesium reacts with the phosphor to form magnesium phosphate, another high temperature phase, providing an additional reinforcing effect, instead of weakening the structure. Hence, the addition of phosphor does not only provide an anti-wetting effect, but assists the maintenance of the refractory structure.

Due to the presence of calcium in the LCC castables calcium phosphate was formed and discreates the positive effect of added aluminium phosphate.

ACKNOWLEDGMENTS

The authors would like to thank the Federation for International Refractory Research and Education (FIRE) for support and Alteo, Gardanne for alumina raw materials supply. Furthermore the authors would like to express their sincere thanks to Kerneos, BASF and Panolin for products provided.

REFERENCES

[1]Gao J., Afshar S., Allaire C.: The corrosion resistance of refractories by molten aluminium *JOM* 1996;**48**(5):23-27.

[2] Brondyke KJ: Effects of molten aluminium on alumina-silica refractories J. Am. Cer. Soc.1953; **36**(5):171-174

[3]Firoozaei E.A., Koshy P.: Effects of $AlPO_4$ addition on the corrosion resistance of andalusite-based low-cement castables with molten Al-alloy, J. Europe. Cer. Soc. 2013,**33**

[4]Praghandeh M., Monshi A., Emadi R.: Effect of Combining Hydraulic Phosphate Bonds on Alumina-Spinel Low Cement Castables, International Journal of ISSI, **Vol.5** 2008,1:31-35

[5]Sarkar R. and Srinivas J.: Effect of Cement and Sol Combined Binders on High-Alumina Refractory Castables, Refractories Worldforum **8**, 2016(4):73-78

[6]Gosh, S. Majumadar R. et al.: Microstructures of refractory castables prepared with sol-gel additives, Ceramic International **29**, 2003:671-677

[7]Gutiérrez-Mora F., Goretta K.C. et al.: High-temperature deformation of amorphous $AlPO_4$-based Nano-composites, Journal of European Ceramic Society **26**, 2006:1179-1183

[8]Tonnesen Th., Loison L., et al.: Refractory Microstructure for a Favourable Infiltration Behaviour against Molten Aluminium Alloys, **59th** International Colloquium on Refractories 2016:182-186

Contact

reichert@ghi.rwth-aachen.de